ISSN 1066-3622, Radiochemistry, 2009, Vol. 51, No. 6, pp. 551–559. © Pleiades Publishing, Inc., 2009.
Original Russian Text © A.Yu. Teterin, M.V. Ryzhkov, Yu.A. Teterin, L. Vukčević, V.A. Terekhov, K.I. Maslakov, K.E. Ivanov, 2009, published in Radiokhimiya, 2009, Vol. 51, No. 6, pp. 481–488.

Nature of Chemical Bonding in ThF_4

A. Yu. Teterin[a], M. V. Ryzhkov[b], Yu. A. Teterin[a], L. Vukčević[c], V. A. Terekhov[d], K. I. Maslakov[a], and K. E. Ivanov[a]

[a] *Russian Research Centre Kurchatov Institute, Moscow, Russia; e-mail: antonxray@yandex.ru, teterin@ignph.kiae.ru*
[b] *Institute of Solid State Chemistry, Ural Branch, Russian Academy of Sciences, Yekaterinburg, Russia*
[c] *University of Montenegro, Podgorica, Montenegro*
[d] *Voronezh State University, Voronezh, Russia*

Received December 29, 2008

Abstract—The fine structure of the X-ray photoelectron spectrum of ThF_4 in the range of valence electrons (binding energy from 0 to 35 eV) is examined. The analysis takes into account the results of theoretical calculation of the electronic structure of the ThF_8^{4-} cluster (point group C_2) as a model of the nearest surrounding of the Th atom in ThF_4, performed by the relativistic discrete variation method. It is demonstrated theoretically and confirmed experimentally that formation of a chemical bond gives rise to filled states of Th5*f* electrons (~0.5 Th5*f* electron) in the energy range of electrons of outer valence molecular orbitals (valence band). The Th6*p* electrons noticeably participate in formation not only of inner valence but also of outer valence (~0.4 Th6*p* electron) molecular orbitals. The composition and order of inner valence molecular orbitals in the energy range from 13 to 35 eV is determined, and the density of states of valence electrons in the range from 0 to 35 eV in ThF_4 is calculated. The results obtained allowed the fine structure of the high-resolution $O_{4,5}$(Th)-emission spectrum of thorium in ThF_4 in the photon energy range from ~60 to ~85 eV, associated with the formation of outer and inner valence molecular orbitals, to be interpreted for the first time.

Key words: thorium tetrafluoride, chemical bonding, X-ray photoelectron spectra

PACS numbers: 33.60.Fy, 71.15.Rf
DOI: 10.1134/S1066362209060010

A study of solid ThF_4 by X-ray photoelectron spectroscopy (XPES) showed that the lines in the range of electron binding energies from 0 to 35 eV have a width of several electron-volts, exceeding in many cases the width of the lines of the electrons from the inner shells [1]. For example, for ThF_4 the full width at half-maximum (FWHM, Γ, eV) of the F1*s* electron line (E_b = 685.5 eV) is Γ = 1.7 eV, whereas FWHM of the F2*s* electron line (E_b = 29.8 eV) is as large as 4 eV, and this line has a structure [1]. This fact contradicts the indeterminacy relationship $\Delta E \Delta\tau \sim h/2\pi$, where ΔE is the natural width of the level from which the photoelectron was removed; $\Delta\tau$, lifetime of the hole state of the ion formed; and h, Planck constant. Indeed, because the hole lifetime ($\Delta\tau$) decreases with an increase in the absolute value of the energy of the given level, for separate atoms the line width in X-ray photoelectron spectra should decrease with a decrease in the electron binding energy. With ThF_4 and other actinide fluorides, however, the pattern is opposite. This fact stimulated extensive theoretical and experimental studies of the nature of chemical bonding in compounds of actinides, in particular, Th. It was found that one of the factors causing line broadening in the X-ray photoelectron spectra in the considered range of actinide electron binding energies in actinide compounds is formation of outer valence molecular orbitals (OVMOs) with the energy from 0 to ~13 eV and inner valence molecular orbitals (IVMOs) with the energies from ~13 to ~50 eV, with effective participation of filled An6*p* atomic shells of actinides [1]. Actually these spectra reflect the structure of the valence band (from 0 to 50 eV) and are observed as bands with a width of several electron-volts. Later it was shown that, under definite conditions, IVMOs can arise in compounds of any elements [1].

Despite the absence of Th5*f* electrons in the Th atom, some experimental [2, 3] and theoretical [3] data for ThO_2 are indicative of the presence in the valence band of this dioxide of filled Th5*f* states. This fact suggests participation of Th5*f* atomic shells in the formation of molecular orbitals in thorium compounds, in particular, in ThF_4. This important conclusion requires confirmation.

The results of qualitative interpretation of the structure of the X-ray photoelectron spectrum of ThF_4 [1] allowed preliminary identification of some lines in the structure of its high-resolution X-ray $O_{4,5}$(Th)-emission spectrum [4]. Correct interpretation of the fine structure of the X-ray photoelectron and X-ray $O_{4,5}$(Th)-emission spectra of ThF_4 was prevented by the lack of the results of relativistic calculations of its electronic structure.

Here we analyze the fine structure of the X-ray photoelectron spectrum of ThF_4 in the range of electron binding energies from 0 to 35 eV and of the high-resolution X-ray $O_{4,5}$(Th)-emission spectrum of ThF_4, taking into account the results of calculations of the electronic structure of the ThF_8^{4-} cluster (point group C_2) as a model of the nearest surrounding of the Th atom in solid ThF_4, performed for the first time by the relativistic discrete variation (RDV) method.

EXPERIMENTAL

The X-ray photoelectron spectrum of ThF_4 was taken on an HP5950A electrostatic spectrometer using monochromated Al$K_{\alpha 1,2}$ X-ray excitation radiation ($h\nu$ = 1486.6 eV) in a vacuum (1.3×10^{-7} Pa) at room temperature [1]. The electrostatic charging of the sample, arising in the course of electron photoemission from its surface, was compensated with a low-energy electron gun. The spectrometer resolution, measured as FWHM of the Au4$f_{7/2}$ electron line, was 0.8 eV. The binding energies E_b (eV) are given relative to the binding energy of C1s electrons of hydrocarbons adsorbed on the sample surface, taken equal to 285.0 eV. On the gold support, E_b(C1s) = 284.7 eV at E_b(Au4$f_{7/2}$) = 83.8 eV. The spectrum of F1s electron line of ThF_4 was observed as a single line with an FWHM (Γ, eV) of 1.7 eV. The width of the C1s electron line of hydrocarbons adsorbed on the sample surface was 1.3 eV. The error in determining the electron binding energies and line widths does not exceed 0.1 eV, and the error in measuring the relative line intensities, 10%.

A ThF_4 sample for an X-ray photoelectron study was prepared from a finely dispersed powder ground in an agate mortar, as a dense thick layer with the mirror-finished surface, pressed into indium on a metallic support. The spectral background caused by elastically scattered electrons was subtracted from the X-ray photoelectron spectrum after Shirley [5].

The X-ray $O_{4,5}$(Th)-emission spectrum of ThF_4, reflecting the Th6p and Th7p,5f states of Th in the valence band, was taken by the primary method with an RSM-500 spectrometer with an energy resolution of 0.3 eV [4]. The ThF_4 spectrum was recorded at an X-ray tube voltage of 3 kV (2 mA) for 60 min. In so doing, variation of the energy of the electrons exciting the spectrum allowed the effective depth of the analysis to be varied from 15 to 50 nm. The area of the excitation electron beam was 5 × 5 mm. The sample was ground in an agate mortar, after which it was ground as a powder into a grooved plate which was fixed using special clamps on the anode of the X-ray tube. A VEU-1 open-type secondary electron multiplier was used for recording the spectrum. A CsI film having a quantum yield in the spectrum region being analyzed was used as a photocathode converting photons into an electron flow. The X-ray $O_{4,5}$(Th) spectrum was recorded three times so as to exclude the effect of changes in the substance composition under an electron beam in a vacuum. The energy positions of the spectrum features in the second reflection order M_ξ were calibrated by recording the lines of Zr (75.55 eV) and Nb (85.85 eV).

CALCULATION PROCEDURE

The ThF_8^{4-} cluster (C_2), reflecting the nearest surrounding of the Th atom in solid ThF_4, is an antiprism with the bases turned by 45° relative to each other. The Th atom is in the center, and the vertices are occupied by eight F atoms (ligands L). The nearest F atoms of the Th surrounding in ThF_4 are subdivided into four nonequivalent groups, each consisting of two atoms, with four different Th–F distances (2.324, 2.317, 2.342, and 2.362 Å); the mean R_{Th-F} distance is 2.336 Å [6].

In this study, for the calculations of this cluster we used for the first time the relativistic discrete variation (RDV) method [7, 8] based on solution of the Dirac–Slater equation for four-component relativistic wavefunctions transforming according to irreducible representations of double point symmetry groups (in this calculation, the symmetry group of the cluster is C_2^*). To obtain symmetrization coefficients, we used an original program implementing the method of projection operators described in detail in [7] and using the matrices of irreducible representations of double groups, obtained in [9]. The extended basis set of numerical atomic four-component atomic orbitals (AOs) obtained by solution of the one-electron problem for isolated neutral atoms included, along with filled orbi-

tals, also unoccupied Th$5f_{5/2}$,$5f_{7/2}$,$7p_{1/2}$,$7p_{3/2}$ states. Numerical Diophantine integration in calculation of matrix elements of the secular equation, which is a characteristic feature of the DV method and is described in detail in [10], was performed over a set of 22 000 points distributed in the cluster space, which ensured no worse than 0.1 eV convergence of the molecular orbital energies. In the calculations we used the local exchange-correlation potential [11]. Because the clusters were fragments of a crystal, in the course of the self-consistence procedure we used the renormalization of the populations of valence AOs of ligands, which allowed us to effectively take into account the stoichiometry of the compound and the charge redistribution between the ligands and surrounding crystal.

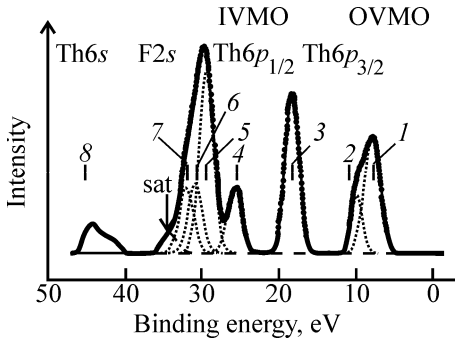

Fig. 1. X-ray photoelectron spectrum of ThF_4. Dotted lines show the spectrum resolution into separate components.

RESULTS AND DISCUSSION

The X-ray photoelectron spectrum of ThF_4 in the binding energy range from 0 to 35 eV can be conventionally subdivided into two parts (Fig. 1). The structure observed in the first part of the spectrum, from 0 to 13 eV, is associated with electrons of OVMOs mainly formed by incompletely filled Th6*d*,7*s*,5*f*,7*p* and F2*p* AOs of the adjacent atoms (Table 1). The fine structure observed in the second part of the spectrum, from 13 to 35 eV, is due to electrons of IVMOs arising largely from strong interaction of electrons of completely filled Th6*p* and F2*s* AOs of the nearest Th and F atoms. The structure of the XPE spectrum of OVMO electrons has characteristic features and can be resolved into two components (*1, 2*). In the region of the IVMO spectrum, there are pronounced maxima, and this region of the spectrum can be resolved into six components (*3*–*8*, Fig. 1). Despite formalism of such spectrum resolution into components, this allows qualitative and quantitative comparison of the XPE spectrum characteristics with the results of calculation of the electronic structure of the ThF_8^{4-} cluster (C_2).

The results of the relativistic calculation of the electronic structure for the ground state of the cluster under consideration and the compositions of molecular orbitals (MOs) are given in Table 1. Because electron photoemission from the molecule results in transition of this molecule into an excited state with a hole on a certain level, for more rigorous comparison of the experimental and theoretical electron binding energies the calculated values for the transition state are used [8]. It is known, however, that, for the valence band, the electron binding energies calculated for the transition state differ from those for the ground state by a constant shift toward higher (in the absolute value) energies. Therefore, in this study, when comparing the calculated and experimental binding energies, the corresponding calculated values were increased in the absolute value by 7.20 eV (Table 2). Taking into account the MO compositions (Table 1) and photoionization cross sections ([12], the σ_i values for Th in Table 1 were calculated by V. G. Yarzhemskii), we determined the theoretical intensities of separate parts of the spectrum (Table 2). When comparing the experimental XPE spectrum and theoretical data, it should be taken into account that the XPE spectrum of ThF_4 reflects the band structure and consists of bands broadened owing to solid-state effects. Despite the approximations used in the calculations, the theoretical and experimental data are in reasonable qualitative agreement. Indeed, the respective widths and relative intensities of lines of the inner and outer valence bands, calculated theoretically and determined from the experimental data, are comparable. Qualitative agreement was obtained between the experimental and calculated binding energies of certain electrons (Table 2). The calculation results obtained in this study and taking into acount relativistic effects practically allow identification of the structure of the XPE spectrum of the ThF_8^{4-} valence electrons in the entire range of binding energies from 0 to 35 eV.

In particular, the intensity of the outer valence band is due to electrons of outer valence Th5*f*,6*d*,7*s*,7*p* and F2*p* AOs of the adjacent atoms and, to a small extent, to electrons of the inner valence U6*p* and F2*s* AOs. The electrons of the Th5*f* states make a noticeable contribution to the intensity of the OVMO electron band (Tables 1, 2). Because these electrons have a high photoionization cross section (Table 1), they can

Table 1. Composition (fractions) and energies E_0 of MOs of the ThF_8^{4-} cluster (C_2) for R_{Th-F} = 2.336 Å (RDV), and photoeffect cross sections σ_i[a] (indicated in parentheses at designations of the corresponding AOs)

MO[b]	$-E_0$, eV[c]	MO composition												
		Th										F		
		6*s* (1.09)	6$p_{1/2}$ (0.89)	6$p_{3/2}$ (1.24)	6$d_{3/2}$ (0.79)	6$d_{5/2}$ (0.74)	7*s* (0.13)	5$f_{5/2}$ (2.74)	5$f_{7/2}$ (2.56)	7$p_{1/2}$ (0.07)	7$p_{3/2}$ (0.09)	2*s* (1.44)	2$p_{1/2}$ (0.13)	2$p_{3/2}$ (0.13)
OVMO														
52$\gamma_{3,4}$	–11.32				0.13	0.69		0.02	0.01			0.03	0.06	0.06
51$\gamma_{3,4}$	–11.16				0.27	0.53		0.01	0.04			0.02	0.03	0.10
50$\gamma_{3,4}$	–10.57				0.10	0.62	0.02	0.06	0.06		0.01	0.02	0.05	0.06
49$\gamma_{3,4}$	–10.28				0.49	0.07	0.06	0.01	0.12	0.11	0.01	0.02	0.02	0.09
48$\gamma_{3,4}$	–9.85				0.13	0.06	0.32	0.01	0.07	0.29	0.04	0.02	0.01	0.05
47$\gamma_{3,4}$	–9.40				0.03	0.02	0.32	0.01	0.05	0.47	0.03	0.03	0.02	0.02
46$\gamma_{3,4}$	–8.67						0.04	0.01	0.02		0.88	0.02		0.03
45$\gamma_{3,4}$	–8.51						0.01	0.05	0.15		0.75	0.01	0.01	0.02
44$\gamma_{3,4}$	–7.85				0.06	0.05		0.03	0.80		0.01		0.01	0.04
43$\gamma_{3,4}$	–6.12				0.09	0.03		0.02	0.78		0.02		0.02	0.04
42$\gamma_{3,4}$	–7.74				0.02	0.06			0.85		0.01		0.01	0.05
41$\gamma_{3,4}$	–7.57							0.02	0.77	0.05	0.10		0.02	0.04
40$\gamma_{3,4}$	–7.36				0.25	0.32	0.11	0.18	0.03				0.02	0.09
39$\gamma_{3,4}$	–7.29				0.08	0.06	0.01	0.72	0.06				0.02	0.05
38$\gamma_{3,4}$	–7.22				0.04	0.05		0.83	0.02		0.01		0.01	0.04
37$\gamma_{3,4}$	–7.10				0.01			0.89		0.01	0.04			0.05
36$\gamma_{3,4}$[d]	0.00			0.08									0.20	0.72
35$\gamma_{3,4}$	0.09			0.01									0.31	0.68
34$\gamma_{3,4}$	0.16												0.30	0.70
33$\gamma_{3,4}$	0.22			0.06				0.01					0.38	0.55
32$\gamma_{3,4}$	0.28			0.01									0.34	0.64
31$\gamma_{3,4}$	0.40												0.34	0.66
30$\gamma_{3,4}$	0.51												0.40	0.60
29$\gamma_{3,4}$	0.64												0.31	0.69
28$\gamma_{3,4}$	0.70			0.01							0.01		0.53	0.45
27$\gamma_{3,4}$	0.78			0.01							0.02		0.29	0.69
26$\gamma_{3,4}$	0.91							0.01	0.01		0.02		0.25	0.71
25$\gamma_{3,4}$	1.10		0.01						0.01	0.02			0.20	0.76
24$\gamma_{3,4}$	1.20							0.02	0.02				0.28	0.68
23$\gamma_{3,4}$	1.23							0.01	0.03				0.38	0.58
22$\gamma_{3,4}$	1.25												0.29	0.70
21$\gamma_{3,4}$	1.30							0.02	0.02				0.31	0.65
20$\gamma_{3,4}$	1.41							0.03	0.02				0.22	0.73
19$\gamma_{3,4}$	1.45							0.01	0.04				0.48	0.47
18$\gamma_{3,4}$	1.85	0.01			0.01	0.01	0.04					0.01	0.33	0.59
17$\gamma_{3,4}$	2.08				0.02	0.09	0.01						0.33	0.54
16$\gamma_{3,4}$	2.12				0.03	0.09						0.01	0.38	0.49
15$\gamma_{3,4}$	2.17				0.08	0.04						0.01	0.20	0.67
14$\gamma_{3,4}$	2.24				0.02	0.11						0.01	0.38	0.48
13$\gamma_{3,4}$	2.30				0.10	0.03			0.01			0.01	0.23	0.63
IVMO														
12$\gamma_{3,4}$	11.20			0.83								0.08	0.03	0.05
11$\gamma_{3,4}$	11.27			0.85								0.07	0.03	0.05
10$\gamma_{3,4}$	17.47		0.53							0.01		0.46		
9$\gamma_{3,4}$	19.07				0.01	0.01						0.97		

Table 1. (Contd.)

MO[b]	$-E_0$, eV[c]	MO composition												
		Th										F		
		6*s* (1.09)	6$p_{1/2}$ (0.89)	6$p_{3/2}$ (1.24)	6$d_{3/2}$ (0.79)	6$d_{5/2}$ (0.74)	7*s* (0.13)	5$f_{5/2}$ (2.74)	5$f_{7/2}$ (2.56)	7$p_{1/2}$ (0.07)	7$p_{3/2}$ (0.09)	2*s* (1.44)	2$p_{1/2}$ (0.13)	2$p_{3/2}$ (0.13)
$8\gamma_{3,4}$	19.18				0.01	0.01						0.97		
$7\gamma_{3,4}$	19.33			0.01	0.01	0.02						0.95		
$6\gamma_{3,4}$	19.42				0.01	0.01	0.02					0.95		
$5\gamma_{3,4}$	19.54					0.01	0.01					0.97		
$4\gamma_{3,4}$	19.77			0.06							0.02	0.92		
$3\gamma_{3,4}$	19.90			0.07							0.02	0.91		
$2\gamma_{3,4}$	20.85		0.45							0.02		0.52		0.01
$1\gamma_{3,4}$	35.15	0.99										0.01		

[a] Photoionization cross sections σ_i (kb per electron) obtained in [12] and by V.G. Yarzhemskii.

[b] MO nos. are decreased by 47, so that $48\gamma_{3,4}$ MO corresponds to $1\gamma_{3,4}$ MO.

[c] The calculated energies are shifted upwards toward positive values by 1.67 eV.

[d] Highest occupied molecular orbital $36\gamma_{3,4}$ (two electrons), the occupation number for $n\gamma_{3,4}$ MOs ($n \le 36$) is 2.

Table 2. Characteristics of the X-ray photoelectron spectrum of ThF_4 and of the ThF_8^{4-} cluster (point group C_2) for R_{Th-F} = 2.336 Å (RDV) and density ρ_i (e^-) of states of Th6*p* and Th5*f* electrons

MO	$-E$,[a] eV	X-ray photoelectron spectrum			Density ρ_i of Th6*p*,5*f* states in e^- (electron) units			
		energy,[b] eV (experiment)	intensity, %					
			theory	experiment	5$f_{5/2}$	5$f_{7/2}$	6$p_{1/2}$	6$p_{3/2}$
OVMO								
$36\gamma_{3,4}$[c]	7.20		1.4					0.16
$35\gamma_{3,4}$	7.29		0.7					0.02
$34\gamma_{3,4}$	7.36		0.6					
$33\gamma_{3,4}$	7.42		1.4		0.02			0.12
$32\gamma_{3,4}$	7.48		0.7					0.02
$31\gamma_{3,4}$	7.60		0.6					
$30\gamma_{3,4}$	7.71		0.6					
$29\gamma_{3,4}$	7.84	7.9(2.1)	0.5	17.7				
$28\gamma_{3,4}$	7.90		0.6					0.02
$27\gamma_{3,4}$	7.98		0.6					0.02
$26\gamma_{3,4}$	8.11		1.0		0.02	0.02		
$25\gamma_{3,4}$	8.30		0.8			0.02	0.02	
$24\gamma_{3,4}$	8.40		0.6		0.04	0.04		
$23\gamma_{3,4}$	8.43		1.4		0.02	0.06		
$22\gamma_{3,4}$	8.45		0.6					
$21\gamma_{3,4}$	8.50		1.4		0.04	0.04		
$20\gamma_{3,4}$	8.61		1.7		0.06	0.04		
$19\gamma_{3,4}$	8.65		1.6		0.02	0.08		
$18\gamma_{3,4}$	9.05		0.8					
$17\gamma_{3,4}$	9.28		1.2					
$16\gamma_{3,4}$	9.32		1.3					
$15\gamma_{3,4}$	9.37		1.3					
$14\gamma_{3,4}$	9.44		1.4					
$13\gamma_{3,4}$	9.50	9.9(1.4)	1.5	6.2		0.02		
$\sum I_i$[d]			24.3	23.9	0.22	0.32	0.02	0.36

Table 2. (Contd.)

MO	$-E$,[a] eV	X-ray photoelectron spectrum			Density ρ_i of Th6*p*,5*f* states in e^- (electron) units			
		energy,[b] eV (experiment)	intensity, %					
			theory	experiment	$5f_{5/2}$	$5f_{7/2}$	$6p_{1/2}$	$6p_{3/2}$
IVMO								
$12\gamma_{3,4}$	18.40	18.4(1.8)	9.4	21.4				1.66
$11\gamma_{3,4}$	18.40		9.5					1.70
$10\gamma_{3,4}$	24.67	25.8(1.9)	6.9	9.0			1.06	
$9\gamma_{3,4}$	26.77		6.1					
$8\gamma_{3,4}$	26.38		6.1					
$7\gamma_{3,4}$	26.53	29.5(1.9)	6.2	24.9				0.02
$6\gamma_{3,4}$	26.62		6.0					
$5\gamma_{3,4}$	26.74		6.1					
$4\gamma_{3,4}$	26.97	31.0(1.9)	6.3	9.4				0.12
$3\gamma_{3,4}$	27.10		6.4					0.14
$2\gamma_{3,4}$	28.05	32.1(1.9)	6.7	8.8			0.90	
Sat		34.2(1.9)		2.6				
$\sum I_i$[d]			75.7	76.1				
$1\gamma_{3,4}$	42.35	44.5(3.7)	8.5[e]	5.8[e]			1.96	3.64

[a] The energies are shifted toward larger values (downwards) by 7.20 eV.

[b] In parentheses are the line widths in eV.

[c] The highest occupied molecular orbital (two electrons), the occupation number for all the orbitals is 2.

[d] Total densities of states of Th6*p* electrons and total line intensities.

[e] Relative to the intensity of the whole spectrum from 0 to 50 eV.

appreciably enhance the intensity of the OVMO electron band. Without taking into account the participation of the Th5*f* states in chemical bonding in ThF_4, the intensity ratio of the OVMO and IVMO electron bands, calculated in the ionic approximation, is 0.24, which is appreciably lower than the experimental value determined in this study, 0.31. With the participation of these electrons in chemical bonding taken into account, the calculated value of this ratio, 0.31, reasonably agrees with the experimental value (Table 2). It should be noted that the calculated relative intensities are given not for the ThF_8^{4-} cluster (C_2) but taking into account that the content of fluorine atoms in ThF_4 is two times smaller (Table 2). It was found that for OVMO and IVMO the relative intensities are 24.3 and 75.7%, respectively, which leads to a somewhat higher value of their ratio (0.32). Practically we obtained an experimental confirmation of the fact that electrons of the Th5*f* states participate in chemical bonding, losing to a minor extent their *f* character. The filled states of these electrons are located on the energy scale in the middle of the outer valence band, and the corresponding unfilled states, in the range from 7.1 to 11.3 eV (Table 1). The filled states of Th6*d* electrons are located mainly at the bottom of the outer valence band. The major contributions to the occupied OVMOs of the cluster are made by the Th5*f* (15.8%), Th6*d* (10.6%), Th6*p* (7.1%), and F2*p* electrons (65.4%), and the remaining Th7*s*,7*p* and F2*s* electrons make a 1.1% contribution. The theoretical and experimental relative intensities for the OVMO and IVMO electrons are comparable, which counts in favor of the approximations we used (Table 2). However, the calculated and experimental relative intensities of IVMO electron lines are poorly consistent, and the range of the experimental energies of the $12\gamma_{3,4}$–$2\gamma_{3,4}$ IVMO electrons of the XPE spectrum, characterizing the width of the spectrum of these electrons, exceeds the corresponding calculated value by 3.95 eV (Table 2).

Taking into account the results of the relativistic calculation of the ThF_8^{4-} cluster (C_2) and the experimental differences between the binding energies of the outer and inner valence electrons of thorium [13], in the MO LCAO approximation it is possible to construct the scheme of molecular orbitals of this cluster (Fig. 2). This scheme allows understanding of the real structure of the XPE spectrum of ThF_4. In this appoximation, we can formally distinguish antibonding [$11,12\gamma_{3,4}$ (3) and $10\gamma_{3,4}$ (4)] and the corresponding

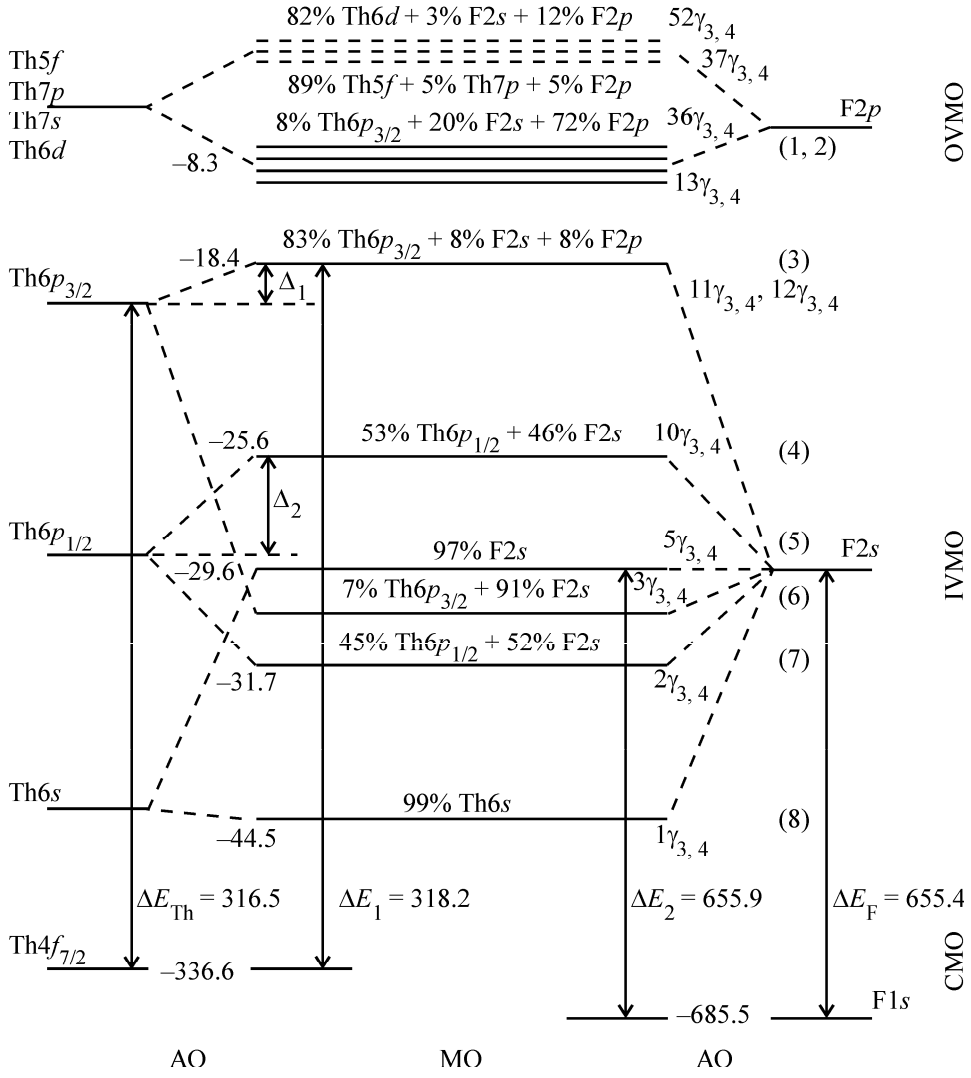

Fig. 2. MO scheme of the ThF_8^{4-} cluster (C_2), constructed taking into account theoretical and experimental data. The chemical shift of the levels in cluster formation from separate atoms is not shown. Arrows denote some experimenally measurable differences between the energies of the levels. In the left part of the figure are the experimental electron binding energies (eV). The energy scale is not consistent.

bonding [3,4$\gamma_{3,4}$ (6) and 2$\gamma_{3,4}$ (7)] IVMOs, and also, to a certain approximation, quasiatomic 9$\gamma_{3,4}$, 8$\gamma_{3,4}$, 7$\gamma_{3,4}$, 6$\gamma_{3,4}$, 5$\gamma_{3,4}$ (5) IVMOs associated mainly with F2*s* electrons. It follows from these experimental data that the energies of the quasiatomic IVMOs associated mainly with F2*s* AOs should be close. Indeed, from the spectrum of the F1*s* electrons of ThF_4 it can be estimated that their chemical nonequivalence should not exceed 0.4 eV, because this line is symmetrical with FWHM Γ = 1.7 eV. The binding energy should be approximately equal to 30.1 eV, because ΔE_F = 655.4 eV and the binding energy of F1*s* electrons in ThF_4 is E_b = 685.5 eV (Fig. 2). The theoretical results are qualitatively consistent with these data. Taking into account that ΔE_{Th} = 316.5 eV, ΔE_1 = 318.2 eV, it can be found that Δ_1 = 1.7 eV. Because the difference between the energies of the 11,12$\gamma_{3,4}$ (3) and 10$\gamma_{3,4}$ (4) IVMO electrons is 7.2 eV and the spin–orbit splitting of the Th6*p* level in the atom ΔE_{sl}(Th6*p*) is 9.2 eV according to the calculation [14] and 9.3 eV according to the experimental data {ΔE_{sl}(Th6*p*) = 7.9 eV [13]}, it can be estimated that the perturbation energy is Δ_2 = 3.8 eV. This value is comparable with the value of 4.0 eV found from the difference between the 10$\gamma_{3,4}$ (4) and 9$\gamma_{3,4}$–5$\gamma_{3,4}$ (5) IVMO electron energies. Hence follows that the energies of the levels of the Th6$p_{1/2}$ and F2*s* elec-

Table 3. Energies of X-ray $O_{4,5}$(Th)-emission Th5*d* ← Th6*p*,7*p*-transitions (eV) in Th and ThF_4, obtained from data of XPES and X-ray emission spectroscopy

Th			ThF_4		
transition	XPES	emission spectrum	transition[a]	XPES	emission spectrum
			$5d_{5/2} \leftarrow 3,4\gamma_{3,4}$ (6)	57.5	?
			$5d_{3/2} \leftarrow 2\gamma_{3,4}$ (7)	63.3	63.3?
			$5d_{3/2} \leftarrow 3,4\gamma_{3,4}$ (6)	64.5	64.5?
$5d_{3/2} \leftarrow 6p_{1/2}$	68.0	–	$5d_{3/2} \leftarrow 10\gamma_{3,4}$ (4)	69.7	67.2, 68.3
$5d_{5/2} \leftarrow 6p_{3/2}$	68.8	–	$5d_{5/2} \leftarrow 11,12\gamma_{3,4}$ (3)	70.1	69.2
$5d_{3/2} \leftarrow 6p_{3/2}$	75.9	–	$5d_{3/2} \leftarrow 11,12\gamma_{3,4}$ (3)	77.1	77.5, 77.0
			$5d_{5/2} \leftarrow$ OVMO (1,2)	80.2	80.5, 83.1
			$5d_{3/2} \leftarrow$ OVMO (1,2)	87.2	

[a] Data for the ThF_8^{4-} cluster (C_2), see Fig. 2.

trons in the Th and F atoms are comparable. However, in this case the antibonding character of the $10\gamma_{3,4}$ (4) IVMO is approximately two times larger than the bonding character (2.3 eV) of the $2\gamma_{3,4}$ (7) IVMO, whereas according to the calculation results these values should be comparable. This is possible in the case if the perturbation Δ_1 is actually considerably smaller. This difference is apparently associated with the IVMO formation, and such a comparison may be not quite correct. Based on the line width of IVMO electrons, it is difficult to make a conclusion about their relative character (bonding or antibonding). It can be assumed, however, that, owing to an impurity of 8% F2*p* AO in $10\gamma_{3,4}$ (4) IVMO, these orbitals partially lose their antibonding character (Tables 1 and 2, Fig. 2, see also [1]).

One of experimental confirmations of the IVMO formation in ThF_4 is the fine structure of its X-ray $O_{4,5}$(Th)-emission spectrum reflecting the bulk of the sample (Fig. 3). Previously we made a preliminary qualitative interpretation of the structure of this spectrum [4]. In this study, the structure of this spectrum was interpreted taking into account the XPES data for ThF_4 and the results of the relativistic calculation of the ThF_8^{4-} cluster (C_2) (Table 3).

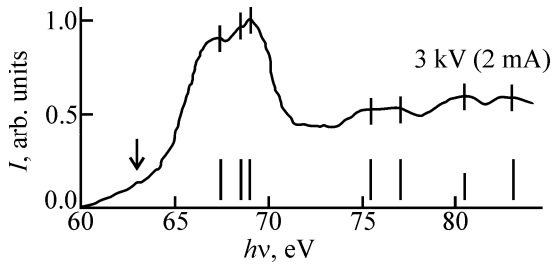

Fig. 3. X-ray $O_{4,5}$(Th)-emission spectrum of thorium, reflecting the Th5*d* ← Th6*p*,7*p*,5*f* transitions in ThF_4. The spectrum was recorded at 3 kV (2 mA) [4].

The thorium X-ray emission spectrum under consideration [4] reflects the electronic transitions $Th5d_{5/2,3/2} \leftarrow Th6p_{3/2,1/2},7p,5f$ [$O_{4,5}$(Th) ← $P_{2,3}O_{VI}$(Th)] in the photon energy range $60 < h\nu < 85$ eV, and its short-wave part overlaps with the absorption spectra [15], which may lead to significant distortion of their shape due to self-absorption (Fig. 3). Previously [15] it was suggested on the basis of Th emission spectra that the long-wave group of lines in such Th spectra is due to the triplet of transitions between the core (inner) shells of Th ions $Th5d_{5/2,3/2} \leftarrow Th6p_{3/2,1/2}$ [$O_{4,5}$(Th) ← $P_{2,3}$(Th)] (Fig. 3, Table 3). However, if only these atomic transitions are taken into account, the effect exerted by the nature of F atoms surrounding the Th atom on the spectrum structure cannot be rationalized, and the fine structure of this emission spectra cannot be satisfactorily interpreted. Therefore, in the interpretation of the fine structure of the emission spectrum under consideration, we took into account the fact that the Th6*p* electron levels in ThF_4 are not inner levels and effectively participate in the IVMO formation [1, 3].

In the emission spectrum of ThF_4, the broad low-energy line is ill-resolved, despite the fact that the apparatus resolution (0.3 eV) is considerably finer than the energy distance between the lines in the energy range from 60 to 76 eV (Fig. 3, Table 3). This fact may be due, in part, to manifestation of additional transitions, not noted in Table 3, in this range of the spectrum.

In the spectrum of ThF_4, there are seven maxima in the energy range 63.3–78.0 eV and pronounced maxima at 80.5 and 83.1 eV. Taking into account the

above suggestions, it can be concluded that the maxima from the first energy range are associated with transitions from IVMOs, and the latter maxima are due to the transition from OVMO to the Th5$d_{5/2}$ level (Fig. 3, Table 3). According to the dipole selection rules ($\Delta l = 1$ and $\Delta j = 0, 1$), the vacancy on the Th5*d* level can be filled with Th6*p*,7*p* or 5*f* electrons of OVMO. This conclusion is consistent with the calculation results which show that the filled OVMOs have an appreciable contribution from both Th6*p* and Th5*f* states. Such reasoning is valid only in the approximation that the molecular orbitals, when formed, preserve partially atomic character. The spectrum under consideration does not allow unambiguous conclusions about the contribution of Th5*f* states to OVMO.

In generation of the emission spectrum of ThF_4, the system in the initial state has a vacancy on the Th5*d* level, and in the final state the vacancy arises on one of the molecular orbitals, whereas in generation of the X-ray photoelectron spectrum the system in the initial state has no vacancies, and in the final state a vacancy is formed on one of inner or molecular levels. This fact can lead to significant differences in the energy characteristics of the spectra under consideration. Therefore, comparison of separate components of the X-ray emission and X-ray photoelectron spectra, made in this study, is tentative (Table 3). This can be done more rigorously taking into account the presently lacking results of precision calculations.

The data obtained show that the structure of the X-ray $O_{4,5}$(Th)-emission spectrum of ThF_4 can be identified only assuming the effective formation of IVMOs in this compound, in particular, with the participation of relatively deeply lying filled Th6*p* and F2*s* AOs of the adjacent atoms.

It should be noted in conclusion that we have examined for the first time the fine structure of the X-ray photoelectron and X-ray $O_{4,5}$(Th)-emission spectra of solid ThF_4 in the energy range from 0 to 35 eV and revealed correspondence between the parameters of the fine structure of these spectra, associated with the electrons of both outer (from 0 to ~13 eV) and inner (from ~13 to ~35 eV) molecular orbitals, largely formed by the Th6*p* and F2*s* shells of the adjacent Th and F atoms, with possible participation of the Th5*f* states.

Practically, on the basis of the X-ray $O_{4,5}$(Th)-emission spectrum we experimentally confirmed the assumed formation of inner valence molecular orbitals in ThF_4. Previously this assumption was made on the basis of considering the fine structure of the X-ray photoelectron spectrum of the electrons from the low-energy filled shells of the adjacent Th and F atoms [1].

ACKNOWLEDGMENTS

The study was financially supported by the Russian Foundation for Basic Research (project nos. 08-03-00 314 and 06-08-00 808) and by the State Program "Leading Scientific Schools" (NSh-616.2008.3).

REFERENCES

1. Teterin, Yu.A. and Teterin, A.Yu., *Usp. Khim*., 2004, vol. 73, no. 6, pp. 588–631.
2. Makarov, L.L., Karaziya, R.I., Batrakov, Yu.F., et al., *Radiokhimiya*, 1978, vol. 20, no. 1, p. 116.
3. Teterin, Yu.A., Ryzhkov, M.V., Teterin, A.Yu., et al., *Nucl. Technol. Radiat. Protect*., 2008, vol. 13, no. 2, pp. 34–42.
4. Teterin, Yu.A., Terekhov, V.A., Teterin, A.Yu., et al., *Dokl. Ross. Akad. Nauk*, 1998, vol. 358, no. 2, pp. 637–640.
5. Shirley, D.A., *Phys. Rev. B*, 1972, vol. 5, no. 12, pp. 4709–4714.
6. Keller, C., *Gmelin Handbuch der anorganischen Chemie. Thorium*, part C1: *Verbindungen mit Edelgasen, Wasserstoff, Sauerstoff*, Berlin: Springer, 1978.
7. Rosen, A. and Ellis, D.E., *J. Chem. Phys*., 1975, vol. 62, no. 8, pp. 3039–3049.
8. Adachi, H., *Technol. Rep. Osaka Univ*., 1977, vol. 27, pp. 569–576.
9. Pyykko, P. and Toivonen, H., *Acta Acad. Aboensis B*, 1983, vol. 43, no. 2, pp. 1–50.
10. Baerends, E.J., Ellis, D.E., and Ros, P., *Chem. Phys*., 1973, vol. 2, no. 1, pp. 41–51.
11. Gunnarsson, O. and Lundqvist, B.I., *Phys. Rev. B*, 1976, vol. 13, no. 10, pp. 4274–4298.
12. Band, I.M., Kharitonov, Yu.I., and Trzhaskovskaya, M.B., *At. Data Nucl. Data Tables*, 1979, vol. 23, pp. 443–505.
13. Fugle, J.S., Burr, A.F., Watsson, L.M., et al., *J. Phys. F: Metal Phys*., 1974, vol. 4, no. 2, pp. 335–342.
14. Huang, K.N., Aojogi, M., Chen, M.N., et al., *At. Data Nucl. Data Tables*, 1976, vol. 18, pp. 243–291.
15. Lyakhovskaya, I.I., Ipatov, V.M., and Zimkina, T.M., *Zh. Strukt. Khim.*, 1977, vol. 18, no. 4, pp. 668–672.